https://doi.org/10.5194/hess-2021-634
Preprint. Discussion started: 18 January 2022

Hydrology and Earth System Sciences
Discussions
Open Access

Effects of the dynamic effective porosity on watertable fluctuations and seawater intrusion in coastal unconfined aquifers

Zhaoyang Luo[1,2,#], Jun Kong[1,3,#], Lili Yao[4], Chunhui Lu[1], Ling Li[5,6], David Andrew Barry[2]

[1]State Key Laboratory of Hydrology-Water Resources and Hydraulic Engineering, Hohai University, Nanjing, China

[2]Ecological Engineering Laboratory (ECOL), Environmental Engineering Institute (IIE), Faculty of Architecture, Civil and Environmental Engineering (ENAC), École Polytechnique Fédérale de Lausanne (EPFL), Lausanne, Switzerland

[3]Key Laboratory of Coastal Disaster and Protection (Ministry of Education), Hohai University, Nanjing, China

[4]Department of Civil, Environmental, and Construction Engineering, University of Central Florida, Orlando, USA

[5]School of Engineering, Westlake University, Hangzhou, China

[6]School of Civil Engineering, The University of Queensland, Brisbane, Australia

[#]Corresponding authors: Zhaoyang Luo (zhaoyang.luo@epfl.ch) and Jun Kong (kongjun999@126.com)

https://doi.org/10.5194/hess-2021-634
Preprint. Discussion started: 18 January 2022

Hydrology and Earth System Sciences
Discussions

Abstract

Watertable fluctuations and seawater intrusion are characteristic features of coastal unconfined aquifers. The dynamic effective porosity due to watertable fluctuations is analyzed and then a modified (empirical) expression is proposed for the dynamic effective porosity based on a dimensionless parameter related to the watertable fluctuation frequency. After validation with both experimental data and numerical simulations, the new expression is implemented in existing Boussinesq equations and a numerical model, allowing for examination of the effects of the dynamic effective porosity on watertable fluctuations and seawater intrusion in coastal unconfined aquifers, respectively. Results show that the Boussinesq equation accounting for the vertical flow in the saturated zone and dynamic effective porosity can accurately predict experimental dispersion relations (that all existing theories fail to predict), highlighting the importance of the dynamic effective porosity in modeling watertable fluctuations in coastal unconfined aquifers. This in turn confirms the utility of the real-valued expression of the dynamic effective porosity. An outcome is that the phase lag between the total moisture (above the watertable) and watertable height measured in laboratory experiments using vertical soil columns (1D systems) can be ignored when predicting watertable fluctuations in coastal unconfined aquifers (2D systems). A dynamic effective porosity that is, by comparison, smaller than the soil porosity leads to a reduction in vertical water exchange between the saturated and vadose zones and hence watertable waves can propagate further landward. The dynamic effective porosity further plays a critical role in simulations of seawater intrusion, since it predicts a more landward seawater-freshwater

interface and a higher position of the upper saline plume.

Keywords: Dynamic effective porosity; Boussinesq equation; watertable fluctuation; dispersion relation; seawater intrusion

https://doi.org/10.5194/hess-2021-634
Preprint. Discussion started: 18 January 2022

Hydrology and Earth System Sciences Discussions

Highlights

- A modified expression is proposed for the dynamic effective porosity due to watertable fluctuations
- The Boussinesq equation correctly predicts watertable fluctuations with involving the vertical flow and dynamic effective porosity
- Numerical models further underestimate seawater intrusion if ignoring the dynamic effective porosity

https://doi.org/10.5194/hess-2021-634
Preprint. Discussion started: 18 January 2022

Hydrology and Earth System Sciences Discussions

1. Introduction

As a transition zone between the ocean and land, coastal unconfined aquifers respond to interactions between terrestrial fresh groundwater and seawater. Due to oceanic oscillations (e.g., tides or waves), water flows into or out of the aquifer periodically, which directly affects a range of groundwater-dependent processes including sediment mobilization, seawater intrusion, submarine groundwater discharge, solute transport and chemical loading to the ocean (e.g., Parlange et al., 1984; Li et al., 1999; Moore, 2010; Xin et al., 2010; Bakhtyar et al., 2011; Werner et al., 2013; Robinson et al., 2018; Wallace et al., 2020). Watertable fluctuations induced by oceanic oscillations are an important signal for quantifying these processes, and their prediction is a longstanding topic (e.g., Philip, 1973; Smiles & Stokes, 1976; Parlange et al., 1984). They are investigated by field measurements (e.g., Nielsen et al., 1990; Raubenheimer et al., 1999; Robinson et al., 2006; Heiss & Michael, 2014; Trglavcnik et al., 2018), laboratory experiments (e.g., Cartwright et al., 2004; Robinson & Li, 2004; Shoushtari et al., 2016, 2017), numerical simulations (e.g., Li et al., 1997; Cartwright et al., 2006; Shoushtari et al., 2015; Brakenhoff et al., 2019) and analytical solutions (e.g., Parlange & Brutsaert, 1987; Barry et al., 1996; Nielsen et al., 1997; Li et al., 2000a,b; Teo et al., 2003; Song et al., 2007; Kong et al., 2013, 2015). Among these, analytical solutions based on the 1D Boussinesq equation describe watertable fluctuations and give results that are easily computed, present explicit relations between parameters that impact watertable fluctuations, and can be used as benchmarks for numerical simulations.

The Dupuit-Forchheimer based Boussinesq equation describes groundwater flow in the

https://doi.org/10.5194/hess-2021-634
Preprint. Discussion started: 18 January 2022

saturated zone (Bear, 2012). It is amenable to analytical investigations, and so is used to reveal mechanisms that influence watertable wave propagation (e.g., Nielsen, 1990; Li et al., 2000a; Teo et al., 2003; Jeng et al., 2005a). To underline the effects of vertical flow on watertable fluctuations, Nielsen et al. (1997) and Liu and Wen (1997) proposed an intermediate-depth Boussinesq equation based on different approximation methods. However, all these investigations ignore unsaturated flow that arises when the watertable rises and falls, which affects predictions of watertable fluctuations (e.g., Gillham, 1984; Kong et al., 2016; Luo et al., 2018). To improve such predictions, modifications to the Boussinesq equation are used. An early step in this direction was taken by Parlange and Brutsaert (1987), who presented a Boussinesq equation that included vertical exchange between the saturated and vadose zones. Barry et al. (1996) presented an approximate analytical solution that considered the effect of this exchange on watertable fluctuations for the case of a periodic boundary condition. Following the method of Parlange and Brutsaert (1987), Jeng et al. (2005b) further improved the Boussinesq model by proposing a higher-order capillarity correction. These modifications were all based on the 1D Boussinesq equation (horizontal flow only) without explicit consideration of the vertical flow (although the effect of the unsaturated zone is considered indirectly). The combined effects of unsaturated and vertical flows were investigated by Li et al. (2000b) and Shoushtari et al. (2016), who extended the intermediate-depth Boussinesq model proposed by Nielsen et al. (1997). Recently, Kong et al. (2013, 2015) developed two types of Boussinesq equation involving horizontal unsaturated flow under the assumption of a hydrostatic vertical pressure distribution, accounting for both short (Kong et al., 2013) and long (Kong et al., 2015) period watertable fluctuations.

When applied to analyze watertable fluctuations in coastal unconfined aquifers subjected to archetypal case of a single-component boundary fluctuation, most of the abovementioned Boussinesq equations predict an asymptotic amplitude decay rate and zero phase lag increase rate (standing wave behavior) of watertable waves for increasing dimensionless aquifer depth, $n_e\omega D/K_s$ (where n_e [-] is the static effective porosity, ω [T^{-1}] is the angular frequency of the boundary forcing, D [L] is the aquifer depth and K_s [LT^{-1}] is the saturated hydraulic conductivity) (e.g., Barry et al., 1996; Liu & Wen, 1997; Nielsen et al., 1997; Li et al., 2000a; Kong et al., 2013, 2015). Nevertheless, the laboratory experiments of Shoushtari et al. (2016), which cover a wide range of $n_e\omega D/K_s$ in an unconfined aquifer with a vertical boundary, indicated an increase of both the amplitude decay rate and phase lag increase rate of watertable waves with increasing $n_e\omega D/K_s$. They concluded that all existing Boussinesq equations cannot predict experimental results correctly. This discrepancy between experimental data and theoretical predictions, especially for the phase lag increase rate, motivates further investigations on the potential mechanisms controlling watertable fluctuations in coastal unconfined aquifers.

Few of the abovementioned Boussinesq equations consider the dynamic effective porosity observed during watertable fluctuations (Nielsen & Perrochet, 2000; Cartwright et al., 2005; Acharya et al., 2012; Pozdniakov et al., 2019). Shoushtari et al. (2016) combined the complex, frequency-dependent effective porosity proposed by Cartwright et al. (2005) with the infinite-order Boussinesq equation of Nielsen et al. (1997), but their new theory failed to predict the experimental results. Therefore, they did not further analyze the effects of the dynamic effective porosity on watertable fluctuations in detail, and it remains unclear whether the dynamic effective porosity affects watertable fluctuations. In addition, as indicated by Hilberts and Troch (2006), the complex-valued expression for the dynamic effective porosity proposed by Cartwright et al. (2005) has limited practical use.

Watertable fluctuations are of additional interest since they affect seawater intrusion behavior in coastal unconfined aquifers. In such aquifers, density-driven flow leads to two different salt areas: a saltwater wedge and an upper saline plume (Robinson et al., 2007). Seawater intrusion under watertable fluctuations is usually investigated numerically (e.g., Brovelli et al., 2007; Xin et al., 2010; Liu et al., 2014; Robinson et al., 2014; Levanon et al., 2016; Yu et al., 2019). Levanon et al. (2017) investigated the responses of seawater intrusion and watertable to surface water level fluctuations combining field measurements with numerical simulations. More recently, Fang et al. (2021) examined the response of seawater intrusion to tide-induced unstable flow using laboratory experiments and numerical simulations. For more information regarding this topic, readers are referred to the comprehensive reviews of Robinson et al. (2018) and Werner et al. (2013). Models of density-dependent flow in coastal aquifers, like the abovementioned Boussinesq models, treat the effective porosity as a constant.

Here, the effects of the dynamic effective porosity effects on watertable fluctuations and seawater intrusion are further explored. First, it is determined empirically from existing experimental measurements and numerical results. Then, modified governing equations that consider the effects of the dynamic effective porosity are proposed to predict watertable fluctuations. This allows for exploration of the underlying mechanisms causing the discrepancy between experimental data and existing theoretical predictions for watertable fluctuations. Since saltwater intrusion is affected by watertable fluctuations, we further examine to what extent the dynamic effective porosity will affect saltwater intrusion in coastal unconfined aquifers based on numerical simulations.

2. Methods

2.1 Original Governing Equations for Watertable Fluctuations

Under the assumption that streamlines are parallel to the underlying bedrock (assumed horizontal) and neglecting unsaturated flow, watertable fluctuations (due, e.g., to tidal forcing) in a coastal unconfined aquifer (supporting information Figure S1) can be described by,

$$n_e \frac{\partial h}{\partial t} = K_s \frac{\partial}{\partial x}\left(h \frac{\partial h}{\partial x} \right) \tag{1}$$

where t [T] is time, x [L] is the horizontal distance from the vertical seaward boundary, and h [L] is the watertable elevation above the aquifer base. Bear (2012) discusses the physical basis of equation (1), often called the Boussinesq equation in groundwater literature (e.g., Hogarth & Parlange, 1999; Parlange et al., 2001). To account for the effects of vertical flow during watertable fluctuations, equation (1) is modified as (Liu & Wen, 1997),

$$n_e \frac{\partial h}{\partial t} = K_s \frac{\partial}{\partial x}\left(h \frac{\partial h}{\partial x} \right) + \frac{K_s D^3}{3} \frac{\partial^4 h}{\partial x^4} \tag{2}$$

Setting $\eta = h - D$ and assuming $\eta \ll D$, equations (1) and (2) are respectively linearized to (Liu & Wen, 1997),

$$n_e \frac{\partial \eta}{\partial t} = K_s D \frac{\partial^2 \eta}{\partial x^2} \tag{3}$$

$$n_e \frac{\partial \eta}{\partial t} = K_s D \left(\frac{\partial^2 \eta}{\partial x^2} + \frac{D^2}{3} \frac{\partial^4 \eta}{\partial x^4} \right) \tag{4}$$

Note that equation (4) is the same as the linearized form of the second-order approximation of Nielsen et al. (1997). For the archetypal case of a single-component sinusoidal tide at the sea boundary (semi-infinite domain, perpendicular beach at the sea boundary, Figure S1), the corresponding dispersion relations of watertable waves for equations (3) and (4) are, respectively (Liu & Wen, 1997; Nielsen et al., 1997; Shoushtari et al., 2016),

$$kD = \sqrt{\frac{n_e \omega D}{K_s} i} \tag{5}$$

$$kD = \sqrt{\frac{3}{2}} \sqrt{-1 + \sqrt{1 + \frac{4}{3} \frac{n_e \omega D}{K_s} i}} \tag{6}$$

where $k = k_r + ik_i$ is the watertable wave number with $i = \sqrt{-1}$. The real ($k_r D$) and imaginary ($k_i D$) parts represent the amplitude spatial decay rate and phase lag increase rate of watertable waves, respectively (Liu & Wen, 1997).

2.2 Relation between the Effective Porosity and Fluctuation Frequency

The effective porosity is defined as the volume of water that an unconfined aquifer releases or gains per unit surface area of aquifer per unit change of the watertable height (Childs, 1960). In most existing Boussinesq equations, the effective porosity is treated as a soil-dependent constant (e.g., Barry et al., 1996; Nielsen et al., 1997; Kong et al., 2013, 2015). However, experimental (Nielsen & Perrochet, 2000; Cartwright et al., 2005), numerical (Acharya et al., 2012; Pazdniakov et al., 2019) and field (Rabinovich et al., 2015) evidence

https://doi.org/10.5194/hess-2021-634
Preprint. Discussion started: 18 January 2022

Hydrology and Earth System Sciences Discussions

indicates that the effective porosity is dynamic and may depend on the porewater velocity. Recently, Pazdniakov et al. (2019) proposed an approximate expression to predict the dynamic effective porosity under seasonal or diurnal groundwater level fluctuations. Motivated by the results of Cartwright et al. (2005) and Pazdniakov et al. (2019) and assuming no truncation of the capillary fringe, we introduce a modified empirical expression to describe the relation between the dynamic effective porosity and fluctuation frequency,

$$n_t = n_e\left[1-\exp\left[-\left(\frac{a}{\tau_\omega}\right)^b\right]\right] \tag{7a}$$

with

$$\tau_\omega = \frac{n_e H_\psi / K_s}{1/\omega} = \frac{n_e \omega H_\psi}{K_s} \tag{7b}$$

$$n_e H_\psi = \int_0^\infty (\theta - \theta_r) d\psi \tag{7c}$$

where n_t [-] is the dynamic effective porosity, τ_ω [-] is a dimensionless parameter related to the watertable fluctuation frequency and soil properties, a [-] and b [-] are the fitting parameters (Section 3.1), θ [-] is the soil water content related to the capillary suction ψ [L], θ_r [-] is the residual soil water content, and H_ψ [L] is a measure of the equivalent saturated height of the unsaturated zone (Parlange & Brutsaert, 1987; Cartwright et al., 2005). Note that equation (7a) has the same functional form as that of Pazdniakov et al. (2019) but a with different variable τ_ω. We will discuss equation (7a) in more detail below.

To solve equation (7c), the relation between θ and ψ is described by a modified van Genuchten model (Troch, 1993; Kong et al., 2016; Luo et al., 2019),

$$\theta = (\theta_s - \theta_r) S_e + \theta_r = (\theta_s - \theta_r)\left[1 + (\alpha_1 \psi)^{n_1}\right]^{-1-1/n_1} + \theta_r \tag{8}$$

https://doi.org/10.5194/hess-2021-634
Preprint. Discussion started: 18 January 2022

Hydrology and Earth System Sciences
Open Access
EGU
Discussions

where θ_s [-] is the saturated soil water content, S_e is the effective saturation, and α_1 [L^{-1}] and n_1 [-] are the parameters obtained by fitting equation (8) to measurements of the soil moisture characteristic curve. Other expressions (e.g., van Genuchten, 1980) can also be used to describe the relation between θ and ψ, but equation (7c) may then need to be evaluated numerically. Observe that the difference between equation (8) and the original van Genuchten (1980) model (VG model) is the exponent, which makes equation (8) integrable to attain simple analytical expression, i.e., substituting equation (8) into equation (7c) leads to,

$$H_\psi = \frac{1}{\alpha_1} \tag{9}$$

By comparison, Pazdniakov et al. (2019) derived τ_ω from the relation between the hydraulic conductivity and the capillary suction, whereas here it is derived from the relation between soil water content and capillary suction. In addition, τ_ω is an approximation in Pozdniakov et al. (2019) (their equation (12)), whereas here it is an exact expression (due to use of equation (8)) related to the fluctuation period and porewater velocity.

2.3 Modified Governing Equations that Consider the Dynamic Effective Porosity

By replacing n_e in equations (3) and (4) with n_t from equation (7a), the governing equations for watertable fluctuations become, respectively,

$$n_e\left[1-\exp\left[-\left(\frac{a}{\tau_\omega}\right)^b\right]\right]\frac{\partial\eta}{\partial t} = K_s D\frac{\partial^2\eta}{\partial x^2} \tag{10}$$

$$n_e\left[1-\exp\left[-\left(\frac{a}{\tau_\omega}\right)^b\right]\right]\frac{\partial\eta}{\partial t} = K_s D\left(\frac{\partial^2\eta}{\partial x^2}+\frac{D^2}{3}\frac{\partial^4\eta}{\partial x^4}\right) \tag{11}$$

The corresponding dispersion relations of watertable waves from equations (10) and (11) are, respectively,

$$kD = \sqrt{\left[1 - \exp\left[-\left(\frac{a}{\tau_\omega}\right)^b\right]\right]\frac{n_e \omega D}{K_s}i} \tag{12}$$

$$kD = \sqrt{\frac{3}{2}}\sqrt{-1 + \sqrt{1 + \frac{4}{3}\left[1 - \exp\left[-\left(\frac{a}{\tau_\omega}\right)^b\right]\right]\frac{n_e \omega D}{K_s}i}} \tag{13}$$

Below, the effects of the dynamic effective porosity on watertable fluctuations will be examined. Consistent with previous studies, possible truncation of the capillary fringe by the soil surface is ignored when examining watertable fluctuations using the Boussinesq equation (e.g., Parlange & Brutsaert, 1987; Barry et al., 1996; Li et al., 2000; Song et al., 2007; Kong et al., 2015).

3. Results and Discussion

3.1. Effects of Watertable Fluctuations on the Dynamic Effective Porosity: 1D Column Experiments

The main reason that the dynamic effective porosity varies with watertable fluctuation rate is the filling/drainage of the unsaturated zone above the aquifer, which is rate-limited due to the water flow rate (Li et al., 1997; Cartwright, 2014). Previous experiments to quantify this exchange used 1D column experiments (Figure S2). For simplicity, readers are referred to Cartwright et al. (2005) for details about the 1D column experiment. To establish the relation between the dynamic effective porosity (n_ω) and forcing fluctuation frequency (ω), the dimensionless parameter τ_ω (equation 7b) is used. Physically, it is the ratio of the response

https://doi.org/10.5194/hess-2021-634
Preprint. Discussion started: 18 January 2022

timescale of the unsaturated zone (n_eH_ψ/K_s, the minimum time needed by the unsaturated zone to fully respond to a boundary disturbance) to the timescale of the surface water level fluctuation imposed on the aquifer ($1/\omega$). If the response time of the unsaturated zone is much longer than the timescale of the surface water level fluctuation (i.e., large τ_ω), the water in the unsaturated zone will not have sufficient time to reach equilibrium during watertable fluctuations. Then, the water exchange between the saturated and unsaturated zones will reduce, thus leading to a smaller n_t. This behavior is consistent with experimental evidence (Cartwright et al., 2005; Cartwright, 2014; Luo et al., 2020) and the complex (dynamic) effective porosity concept of Nielsen and Perrochet. (2000) and Cartwright et al. (2005). Equation (7a) captures this behavior since n_t approaches n_e for small τ_ω, whereas it tends to zero for large τ_ω.

The appropriateness of the functional form of equation (7a) is checked by fitting it to n_t obtained from experiments and numerical simulations. Using the similar experimental apparatus presented in Figure S2, Cartwright et al. (2005) carried out 63 experiments involving three different soils. For simplicity, readers are referred to Cartwright et al. (2005) for more details about the experiments. As can be seen from Figure 1a, the range of n_t/n_e and τ_ω for these experiments varies from $10^{-2.5}$ to $10^{-0.4}$ (two orders of magnitude) and 10^{-2} to 10^{3} (five orders of magnitude), respectively. As expected, n_t/n_e declines with increasing τ_ω. In addition, regardless of soil type there is a clear relation between n_t/n_e and τ_ω, which can be fitted (MATLAB© ver. 9 function "lsqcurvefit") by equation (7a) with a = 0.0335 and b = 0.4444 (Figure 1a). In general, equation (7a) performs well although there is small deviation

https://doi.org/10.5194/hess-2021-634
Preprint. Discussion started: 18 January 2022

between equation (7a) and experimental data at larger τ_ω. The fitted values match well with the experimental values (R^2 = 0.94), indicating that equation (7a) satisfactorily describes the dynamic effective porosity as it varies with the fluctuation frequency for different soils.

Since the ranges of n_t/n_e and τ_ω obtained from experiments are relatively narrow, we consider also the numerical simulations of Pozdniakov et al. (2019). A total of 299 cases covering 100 random soils was simulated with HYDRUS 1D (Šimůnek et al., 2020). Compared with available experiments, these numerical simulations cover wider ranges of n_t/n_e and τ_ω, with the former varying from 10^{-3} to 10^0 (three orders of magnitude) and the latter from 10^{-3} to 10^5 (eight orders of magnitude). As shown in Figure 2a, n_t/n_e is equal to unity at small τ_ω and then decreases rapidly with increasing τ_ω, suggesting a frequency-dependent n_t/n_e. Again, numerical results show a clear dependence of n_t/n_e on τ_ω although both n_t/n_e and τ_ω span a broad range. For the numerical model results, the relation between n_t/n_e and τ_ω can be approximated by equation (7a) with a small deviation at large τ_ω taking a = 0.1216 and b = 0.3642. We also plotted the fitted n_t/n_e versus numerical n_t/n_e (Figure 2b). The fitted values match well with the numerical values (R^2 = 0.98).

Based on the experimental and numerical data, the effective porosity will be significantly impacted by watertable fluctuations when τ_ω is larger than 0.01 (green dashed line in Figures 1a and 2a). This gives a critical value to identify whether the unsaturated zone has sufficient time to respond to a boundary fluctuation. It is worth noting that the values of a and b are different for experimental and numerical results, which leads to a small deviation between the optimal fitting curves (Figure 2a). This systematic deviation could be induced by

https://doi.org/10.5194/hess-2021-634
Preprint. Discussion started: 18 January 2022

Hydrology and Earth System Sciences
Discussions

either the experiments or the simulations. On the one hand, hysteresis is ignored in the numerical simulations. On the other hand, there is a lack of measurements for n_t/n_e close to 1 for experiments, which will affect the fitting results. In addition, a linear response of the watertable is assumed to determine the experimental dynamic effective porosity (Cartwright et al., 2005), i.e., the governing equation was linearized above under the assumption of a small amplitude fluctuation, which may contribute to the deviation. Overall, despite these uncertainties, the relation between the dynamic effective porosity and fluctuation frequency can be predicted by equation (7a). In practice, we suggest that the fit of equation (7a) to the experimental data is preferred.

Both the 1D sand column experiments carried out by Nielsen and Perrochet (2000) and Cartwright et al. (2005) indicate a phase lag between the total moisture (above the watertable) and watertable height during watertable fluctuations. In order to account for this phase lag, Cartwright et al. (2005) suggested a complex-valued expression, where the real and imaginary parts respectively represent the effective porosity and phase lag, to describe the dynamic effective porosity. However, in this study, we focus on watertable fluctuations in coastal unconfined aquifers (2D systems) as they respond boundary forcing with a fixed frequency, not the moisture content above the watertable. For this case, in the following section we examine the impact of equation (7a) in predicting watertable fluctuations in careful 2D experiments for horizontal transmission of watertable fluctuations forced by a single-component watertable change at the boundary.

https://doi.org/10.5194/hess-2021-634
Preprint. Discussion started: 18 January 2022

3.2. Effects of the Dynamic Effective Porosity on Watertable Fluctuations: 2D Aquifer Experiments

Here, we use an extensive set of existing 2D experimental results to examine the effects of the dynamic effective porosity on watertable fluctuations. Specifically, the combination of equation (7a) with existing Boussinesq equations produced modified governing equations, equations (10) and (11), which can be used to predict the effects of the dynamic effective porosity on watertable wave propagation in coastal unconfined aquifers. Following previous studies (e.g., Nielsen, 1990; Barry et al., 1996; Li et al., 2000a; Cartwright et al., 2004; Kong et al., 2015), the dispersion relation linking the amplitude decay rate (k_rD) with phase lag increase rate (k_iD), is adopted to characterize the propagation of watertable waves. A total of 122 sand flume experiments, covering a wide range of $n_e\omega D/K_s$ values, were conducted by Shoushtari et al. (2016) and are used here to examine the validity of these predictions. The experiments were carried out in a sand flume with dimensions of 9 m (length) × 0.15 m (width) × 1.5 m (height). Readers are referred to Shoushtari et al. (2016) for details about the sand flume experiment. Since the properties are similar, the two sands adopted in Shoushtari et al. (2016)'s experiments are considered to have the same VG fitting parameters (van Genuchten, 1980). As can be seen from Figure 3a, equation (8) matches well with the VG model based on the parameters listed in Table 1.

Figure 4 of Shoushtari et al. (2016) shows the predictions of the dispersion relations in equations (5) and (6), which were derived from equations (3) and (4), respectively. Specifically, their Figure 4 plots predicted k_rD vs k_iD curves and experimental data. Equation

https://doi.org/10.5194/hess-2021-634
Preprint. Discussion started: 18 January 2022

(5) performs poorly whereas equation (6) compares well with the data. Note that plots of k_rD vs k_iD are independent of any specific form selected for n_e since such plots depend on a single dimensionless parameter, $n_e\omega D/K_s$ (Nielsen et al., 1997; Shoushtari et al., 2016). The role of $n_e\omega D/K_s$ is instead explored by examining each of k_rD and k_iD as a function of $n_e\omega D/K_s$, as done in Figure 4, to check the applicability of the modified equations (10) and (11) (i.e., approximate analytical solutions of the dispersion relation shown in equations (13) and (14), respectively). Since there is a small deviation between the best-fit curves for the experimental and numerical data of n_t/n_e and τ_ω, two pairs of curves for the two pairs of best-fit a and b values are compared: one pair of values obtained from fitting to experimental data and another pair obtained from fitting to numerical data. In contrast to the relation between k_rD and k_iD (which, as mentioned, is independent of the functional form of n_e), there are large deviations between predictions of k_rD and k_iD as they vary with $n_e\omega D/K_s$ from governing equations with or without considering the dynamic effective porosity effects, depending on the values of a and b. Moreover, these deviations increase for increasing $n_e\omega D/K_s$. Again, this emphasizes that the effective porosity is increasingly influenced by watertable fluctuations as $n_e\omega D/K_s$ increases. Compared to the original equations (3) and (4) (i.e., approximate analytical solutions of the dispersion relation shown in equations (5) and (6), respectively) that assume a constant effective porosity, for a given $n_e\omega D/K_s$, both k_rD and k_iD are smaller when the dynamic effective porosity is considered. This is because a smaller effective porosity corresponds to reduced vertical water exchange and hence watertable waves can propagate further landward, i.e., smaller k_rD and k_iD (Li et al., 2000b).

https://doi.org/10.5194/hess-2021-634
Preprint. Discussion started: 18 January 2022

Hydrology and Earth System Sciences
Discussions

Shoushtari et al. (2016) analyzed their experimental results and demonstrated that all existing theories are unable to predict the measured dispersion relation correctly (Figure S3 in supporting information and Figure 5 in Shoushtari et al. (2016)), even considering different factors (e.g., capillary effect, hysteresis, porous media deformation (Shoushtari & Cartwright, 2017)). In contrast, equation (11) predicts well the relations between k_rD or k_iD and $n_e\omega D/K_s$, despite the fact that experimental and numerical results do not agree (and give rise to different values of *a* and *b*). The success of equation (11) highlights the significant role played by the dynamic effective porosity on watertable fluctuations, and so confirms that equation (7a) fitted by nonlinear least squares can be used to describe the relation between the dynamic effective porosity and fluctuation frequency. Moreover, this in turn suggests that the phase lag between the total moisture and watertable height measured in laboratory experiments using vertical soil columns can be ignored when predicting watertable fluctuations. It should be noted that substituting the complex-valued expression for the dynamic effective porosity proposed by Cartwright et al. (2005) into equation (2) cannot predict the measured dispersion relation well (Figure S4). Furthermore, experiments conducted by Parlange et al. (1984) and Cartwright et al. (2003) were used to check the validity of equation (11). As can be seen from Figures 5 and 6, predictions of equation (11) agree well with the measured watertable in both experiments. The analytical solution of *h* is given in Appendix based on the dispersion relation.

By comparison, equation (11) with *a* and *b* from experiments (a = 0.0335 and b = 0.4444) performs better than the corresponding simulation-derived values in predicting

https://doi.org/10.5194/hess-2021-634
Preprint. Discussion started: 18 January 2022

experimental results of Shoushtari et al. (2016) and Cartwright et al. (2003). Therefore, the experimentally-determined values of *a* and *b* are recommended for practical use when predicting watertable fluctuations in coastal unconfined aquifers.

3.3. Effects of the Dynamic Effective Porosity on Seawater Intrusion

As seen above, the dynamic effective porosity and watertable fluctuations are functionally related, especially for high frequency fluctuations. Therefore, one would intuitively anticipate that the dynamic effective porosity will also influence seawater intrusion in coastal unconfined aquifers. To explore the influence of the effects of the dynamic effective porosity on seawater intrusion, we use SUTRA, a 3D variable-saturation and variable-density groundwater model (Voss & Provost, 2008).

Numerical simulations were carried out for the experiment of Shen et al. (2020), who investigated seawater intrusion under watertable fluctuation influences in a sand flume with dimensions of 7.7 m (length) × 1.2 m (height) × 0.16 m (width). Figure S5 illustrates the numerical model geometry for the base case, as well as relevant numerical settings. Again, equation (8) matches perfectly the VG model of Shen et al. (2020) (Figure 3b, parameters listed in Table 1). A high-frequency water level fluctuation with a period of 240 s was imposed at the sea boundary, leading to dynamic effective porosities of 0.12 and 0.2 computed using the pairs of *a* and *b* obtained above by fitting equation (7a) to experimental and numerical data, respectively (the static effective porosity is 0.4, Table 1). Only the effective porosity is changed while other parameters are fixed for these two cases. All numerical simulations were run for 26 h, with a time step of 4 s. The model domains were

https://doi.org/10.5194/hess-2021-634
Preprint. Discussion started: 18 January 2022

Hydrology and Earth System Sciences
Discussions

discretized with node spacings of 0.02 and 0.1 m in the horizontal and vertical directions, respectively, to satisfy the Péclet number stability criterion (Voss & Souza, 1987). Different mesh schemes were tested to ensure mesh-independent numerical results. The transient locations of the saltwater wedge and upper saline plume were observed to ensure quasi-steady state results, defined as when the locations of the saltwater wedge and upper saline plume remain unchanged after one period. The direct solver in SUTRA (DIRECT) was adopted in the numerical simulations with convergence tolerances of 10^{-10} kg/m/s^2 and 10^{-10} for solver iterations during pressure and transport solutions, respectively.

Figure 7 compares the experimental and numerical results, which show two different salt areas under tidal forcing: a saltwater wedge and an upper saline plume. For the base case with $n_t = 0.4$ (without considering the dynamic effective porosity, Figure 7b), the numerical model significantly underestimates the seawater-freshwater interface location while it overestimates the area of upper saline plume. Once the dynamic effective porosity is considered, however, the numerical model performs much better in predicting seawater intrusion. For the case with $n_t = 0.2$ (a and b obtained by fitting equation (7a) to numerical data, Figure 7c), the numerical model predicts almost the same magnitude of the upper saline plume as the experiment, despite a small deviation for the seawater-freshwater interface location. In contrast, the numerical model with $n_t = 0.12$ (a and b obtained by fitting equation (7a) to experimental data, Figure 7d) predicts more accurately the seawater-freshwater interface location, while it slightly underestimates the area of the area of upper saline plume. These results highlight the importance of including the dynamic effective porosity in numerical models for assessing

https://doi.org/10.5194/hess-2021-634
Preprint. Discussion started: 18 January 2022

saltwater intrusion. Since the location of the saltwater wedge is more important for coastal groundwater management, the experimentally-determined values of *a* and *b* are also recommended for practical use when predicting seawater intrusion in coastal unconfined aquifers.

Observe that a smaller effective porosity leads to a more landward seawater-freshwater interface with a higher position of the upper saline plume (Figure 7a). In the governing flow equation used in the numerical solution, a decrease of the effective porosity is equivalent to an increase of the hydraulic conductivity. As a result, the seawater-freshwater interface moves more landward while the upper saline plume moves toward a higher position. Note that a landward movement of the bottom saltwater wedge will push the upper saline plume upward to maintain the outward flow of inland freshwater. Regardless of the values of *a* and *b* obtained from fitting equation (7a) to measured or numerical data, the numerical results match well with the experiments (Figure 7a). This again confirms that equation (7a) fitted by nonlinear least squares can be used to describe the relation between the dynamic effective porosity and fluctuation frequency. Again, this suggests that the phase lag between the total moisture and watertable height measured in laboratory experiments using vertical soil columns can be ignored when predicting seawater intrusion.

In reality, wave-dominated unconfined aquifers are widely distributed along the coast (e.g., Xin et al., 2010; Robinson et al., 2014). Additionally, high-frequency fluctuations are usually adopted at the sea boundary when conducting seawater intrusion experiments (e.g., Kuan et al., 2012; Yu et al., 2019; Shen et al., 2020). Under these conditions, neglecting the

https://doi.org/10.5194/hess-2021-634
Preprint. Discussion started: 18 January 2022

dynamic effective porosity will lead to an inappropriate estimation of seawater intrusion based on numerical models. Zhang et al. (2016) found that only an increase of K_s (from 17.28 to 132.3 m/d, one order of magnitude larger) enabled their model to perform well in predicting groundwater flow and seawater intrusion in a field aquifer. Our results suggest that, in part at least, this increase in K_s is due to their neglect of the dynamic effective porosity since, as mentioned earlier, an increase of K_s is equivalent to a decrease of n_t in numerical models.

4. Conclusions

This study evaluates the effects of the dynamic effective porosity on watertable fluctuations and seawater intrusion in coastal unconfined aquifers. Following Pazdniakov et al. (2019), we propose a new modified expression to predict the dynamic effective porosity under watertable fluctuations. After validating against both experiments and numerical simulations, this expression is coupled with existing governing equations and a numerical model to examine the effects of the dynamic effective porosity on watertable fluctuations and seawater intrusion, respectively. The results lead to the following conclusions:

(1) The new modified expression is able to predict the dynamic effective porosity accurately during watertable fluctuations. Moreover, coupling this real-valued expression of the dynamic effective porosity with existing governing equations leads to accurate predictions of watertable fluctuations, suggesting the phase lag between the total moisture (above the watertable) and watertable height measured in laboratory experiments using vertical soil columns (1D systems) can be ignored when predicting watertable fluctuations in coastal

unconfined aquifers (2D systems). In other words, this work demonstrates that a real-valued expression for the dynamic effective porosity is sufficient for practical use.

(2) The modified governing equation taking into account the vertical flow in the saturated zone and dynamic effective porosity can accurately predict experimental dispersion relations, highlighting the importance of the dynamic effective porosity in modeling watertable fluctuations. For a given soil, the dynamic effective porosity decreases with increasing fluctuation frequency, leading to a decrease in vertical water exchange between the saturated zone and unsaturated zone and hence watertable waves can propagate further landward, especially for high frequency fluctuations.

(3) In addition to watertable fluctuations, the dynamic effective porosity further plays an important role in controlling seawater intrusion. As confirmed by laboratory experimental data, by including the dynamic effective porosity, the numerical model predicts a more landward seawater-freshwater interface and a higher position of the upper saline plume. This suggests that neglecting the dynamic effective porosity leads to inappropriate estimations of seawater intrusion in coastal unconfined aquifers.

The empirical expression for the dynamic effective porosity proposed here is based on numerical results, and data from 1D sand column experiments. More measured data, obtained under a variety of conditions, would be helpful to further examine the expression for the dynamic effective porosity. For example, the dynamic effective porosity could be related to pore water velocity given that the boundary signal is usually irregular (combination of tides and waves), and the watertable fluctuation amplitude. Although uncertainties due to these

https://doi.org/10.5194/hess-2021-634
Preprint. Discussion started: 18 January 2022

factors could provide further insights, despite its empirical basis this study shows that the dynamic effective porosity plays an important role in modeling watertable fluctuations and seawater intrusion. The real-valued effective porosity model presented here leads to reliable predictions of groundwater response, which is essential for understanding many groundwater-dependent processes in coastal unconfined aquifers.

https://doi.org/10.5194/hess-2021-634
Preprint. Discussion started: 18 January 2022

Hydrology and Earth System Sciences Discussions

Appendix

Assuming a single-component sinusoidal tide at the sea boundary, we have,

$$h(0,t) = D + A\sin(\omega t) \tag{A1}$$

Based on the dispersion relation, the analytical solution of h is (Parlange & Brutsaert, 1987),

$$h = D + A\exp(-k_r Dx)\sin(\omega t - k_i Dx) \tag{A2}$$

https://doi.org/10.5194/hess-2021-634
Preprint. Discussion started: 18 January 2022

Code/Data availability

The paper is theoretical, and data used in this study can be found in Parlange et al. (1984), Cartwright et al. (2003, 2005), Shoushtari et al. (2016), Pozdniakov et al. (2019) and Shen et al. (2020).

https://doi.org/10.5194/hess-2021-634
Preprint. Discussion started: 18 January 2022

Hydrology and Earth System Sciences
Discussions

Author contribution

All authors contributed to the design of the research. ZL carried out data collation, developed the theories and prepared the manuscript with contributions from all co-authors. All authors contributed to the interpretation of the results and provided feedback.

https://doi.org/10.5194/hess-2021-634
Preprint. Discussion started: 18 January 2022

Hydrology and Earth System Sciences
Discussions

Competing interests

The authors declare that they have no conflict of interest.

Acknowledgments

This research was supported by the National Natural Science Foundation of China (51979095) and Marine Science and Technology Innovation Project of Jiangsu (JSZRHYKJ202105). ZL acknowledges EPFL for financial support and JK acknowledges the Qing Lan Project of Jiangsu Province (2020). We gratefully appreciate N. Cartwright for providing the experimental data of Shoushtari et al. (2016), P. Wang for providing the numerical data of Pozdniakov et al. (2019), and Y. Shen for providing the experimental data of Shen et al. (2020).

https://doi.org/10.5194/hess-2021-634
Preprint. Discussion started: 18 January 2022

References

Acharya, S., Jawitz, J. W., & Mylavarapu, R. S. (2012). Analytical expressions for drainable and fillable porosity of phreatic aquifers under vertical fluxes from evapotranspiration and recharge. *Water Resources Research*, *48*(11), W11526. https://doi.org/10.1029/2012WR012043

Bakhtyar, R., Brovelli, A., Barry, D. A., & Li, L. (2011). Wave-induced water table fluctuations, sediment transport and beach profile change: Modeling and comparison with large-scale laboratory experiments. *Coastal Engineering*, *58*(1), 103–118. https://doi.org/10.1016/j.coastaleng.2010.08.004

Barry, D. A., Barry, S. J., & Parlange, J.-Y. 1996. Capillarity correction to periodic solutions of the shallow flow approximation, In *Mixing Processes in Estuaries and Coastal Seas*, *C. B. Pattiaratchi (editor), Coastal and Estuarine Studies*, Volume 50, American Geophysical Union, Washington, DC, pp. 496–510. https://doi.org/10.1029/CE050.

Bear, J. (2012). *Hydraulics of Groundwater*. Dover Publications, Inc., Mineola, New York.

Brakenhoff, L. B., Smit, Y., Donker, J. J. A., & Ruessink, G. (2019). Tide-induced variability in beach surface moisture: Observations and modelling. *Earth Surface Processes and Landforms*, *44*(1), 317–330. https://doi.org/10.1002/esp.4493

Brovelli, A., Mao, X., & Barry, D. A. (2007). Numerical modeling of tidal influence on density-dependent contaminant transport. *Water Resources Research*, *43*(10), W10426. https://doi.org/10.1029/2006WR005173

Cartwright, N. (2014). Moisture-pressure dynamics above an oscillating water table. *Journal* *of Hydrology*, *512*, 442–446. https://doi.org/10.1016/j.jhydrol.2014.03.024

Cartwright, N., Jessen, O. Z., & Nielsen, P. (2006). Application of a coupled ground-surface water flow model to simulate periodic groundwater flow influenced by a sloping boundary, capillarity and vertical flows. *Environmental Modelling & Software*, *21*(6), 770–778. https://doi.org/10.1016/j.envsoft.2005.02.005

Cartwright, N., Nielsen, P., & Dunn, S. (2003). Water table waves in an unconfined aquifer: Experiments and modeling. *Water Resources Research*, *39*(12), 1330. https://doi.org/10.1029/2003WR002185

Cartwright, N., Nielsen, P., & Li, L. (2004). Experimental observations of watertable waves in an unconfined aquifer with a sloping boundary. *Advances in Water Resources*, *27*(10), 991–1004. https://doi.org/10.1016/j.advwatres.2004.08.006

Cartwright, N., Nielsen, P., & Perrochet, P. (2005). Influence of capillarity on a simple harmonic oscillating water table: Sand column experiments and modeling. *Water Resources Research*, *41*(8), W08416. https://doi.org/10.1029/2005WR004023

Childs, E. C. (1960). The nonsteady state of the water table in drained land. *Journal of Geophysical Research*, *65*(2), 780–782. https://doi.org/10.1029/JZ065i002p00780

Fang, Y., Zheng, T., Zheng, X., Yang, H., Wang, H., & Walther, M. (2021). Influence of tide-induced unstable flow on seawater intrusion and submarine groundwater discharge. *Water Resources Research*, *57*(4), e2020WR029038. https://doi.org/10.1029/2020WR029038

Gillham, R. W. (1984). The capillary fringe and its effect on water-table response. *Journal of*

Hydrology, *67*(1–4), 307–324. https://doi.org/10.1016/0022-1694(84)90248-8

Heiss, J. W., & Michael, H. A. (2014). Saltwater-freshwater mixing dynamics in a sandy beach aquifer over tidal, spring-neap, and seasonal cycles. *Water Resources Research*, *50*(8), 6747–6766. https://doi.org/10.1002/2014WR015574

Hilberts, A. G. J., & Troch, P. A. (2006). Comment on "Influence of capillarity on a simple harmonic oscillating water table: Sand column experiments and modeling" by Nick Cartwright et al. *Water Resources Research*, *42*(11), W11601. https://doi.org/10.1029/2006WR005042

Hogarth, W. L., & Parlange, J.-Y. (1999). Solving the Boussinesq equation using solutions of the Blasius equation. *Water Resources Research*, *35*(3), 885–887. https://doi.org/10.1029/1998WR900082

Jeng, D.-S., Mao, X., Enot, P., Barry, D. A., & Li, L. (2005a). Spring-neap tide-induced beach water table fluctuations in a sloping coastal aquifer. *Water Resources Research*, *41*(7), W07026. https://doi.org/10.1029/2005WR003945

Jeng, D.-S., Seymour, B. R., Barry, D. A., Li, L., & Parlange, J.-Y. (2005b). New approximation for free surface flow of groundwater: Capillarity correction. *Advances in Water Resources*, *28*(10), 1032–1039. https://doi.org/10.1016/j.advwatres.2004.05.012

Kong, J., Shen, C., Luo, Z., Hua, G., & Zhao, H. (2016). Improvement of the hillslope-storage Boussinesq model by considering lateral flow in the unsaturated zone. *Water Resources Research*, *52*(4), 2965–2984. https://doi.org/10.1002/2015WR018054

https://doi.org/10.5194/hess-2021-634
Preprint. Discussion started: 18 January 2022

Hydrology and Earth System Sciences
Discussions

Kong, J., Shen, C.-J., Xin, P., Song, Z., Li, L., Barry, D. A., Jeng, D.-S., Stagnitti, F., Lockington, D. A., & Parlange, J.-Y. (2013). Capillary effect on water table fluctuations in unconfined aquifers. *Water Resources Research*, *49*(5), 3064–3069. https://doi.org/10.1002/wrcr.20237

Kong, J., Xin, P., Hua, G.-F., Luo, Z.-Y., Shen, C.-J., Chen, D., & Li, L. (2015). Effects of vadose zone on groundwater table fluctuations in unconfined aquifers. *Journal of Hydrology*, *528*, 397–407. https://doi.org/10.1016/j.jhydrol.2015.06.045

Kuan, W. K., Jin, G., Xin, P., Robinson, C., Gibbes, B., & Li, L. (2012). Tidal influence on seawater intrusion in unconfined coastal aquifers. *Water Resources Research*, *48*(2), W02502. https://doi.org/10.1029/2011WR010678

Levanon, E., Shalev, E., Yechieli, Y., & Gvirtzman, H. (2016). Fluctuations of fresh-saline water interface and of water table induced by sea tides in unconfined aquifers. *Advances in Water Resources*, *96*, 34–42. https://doi.org/10.1016/j.advwatres.2016.06.013

Levanon, E., Yechieli, Y., Gvirtzman, H., & Shalev, E. (2017). Tide-induced fluctuations of salinity and groundwater level in unconfined aquifers–Field measurements and numerical model. *Journal of Hydrology*, *551*, 665–675. https://doi.org/10.1016/j.jhydrol.2016.12.045

Li, L., Barry, D. A., & Stagnitti, F. (2000a). Beach water table fluctuations due to spring-neap tides: Moving boundary effects. *Advances in Water Resources, 23*(8), 817–824. https://doi.org/10.1016/S0309-1708(00)00017-8

https://doi.org/10.5194/hess-2021-634
Preprint. Discussion started: 18 January 2022

Li, L., Barry, D. A., Stagnitti, F., & Parlange, J.-Y. (2000b). Groundwater waves in a coastal aquifer: A new governing equation including vertical effects and capillarity. *Water Resources Research*, *36*(2), 411–420. https://doi.org/10.1029/1999WR900307

Li, L., Barry, D. A., Stagnitti, F., & Parlange, J.-Y. (1999). Submarine groundwater discharge and associated chemical input to a coastal sea. *Water Resources Research*, *35*(11), 3253–3259. https://doi.org/10.1029/1999WR900189

Li, L., Barry, D. A., Parlange, J.-Y., & Pattiaratchi, C. B. (1997). Beach water table fluctuations due to wave run-up: Capillarity effects. *Water Resources Research, 33*(5), 935–945. https://doi.org/10.1029/96WR03946

Liu, Y., Mao, X., Chen, J., & Barry, D. A. (2014). Influence of a coarse interlayer on seawater intrusion and contaminant migration in coastal aquifers. *Hydrological Processes*, *28*(20), 5162–5175. https://doi.org/10.1002/hyp.10002

Liu, P. L. F., & Wen, J. (1997). Nonlinear diffusive surface waves in porous media. *Journal of Fluid Mechanics*, *347*, 119-139. https://doi.org/10.1017/S0022112097006472

Luo, Z., Kong, J., Ji, Z., Shen, C., Lu, C., Xin, P., Zhao, Z., Li, L., & Barry, D. A. (2020). Watertable fluctuation-induced variability in the water retention curve: Sand column experiments. *Journal of Hydrology*, *589*, 125125. https://doi.org/10.1016/j.jhydrol.2020.125125

Luo, Z., Kong, J., Shen, C., Lu, C., Hua, G., Zhao, Z., Zhao, H., & Li, L. (2019). Evaluation and application of the modified van Genuchten function for unsaturated porous media. *Journal of Hydrology*, *571*, 279–287. https://doi.org/10.1016/j.jhydrol.2019.01.051

https://doi.org/10.5194/hess-2021-634
Preprint. Discussion started: 18 January 2022

Hydrology and Earth System Sciences Discussions
Open Access
EGU

Luo, Z., Shen, C., Kong, J., Hua, G., Gao, X., Zhao, Z., Zhao, H., & Li, L. (2018). Effects of unsaturated flow on hillslope recession characteristics. *Water Resources Research*, *54*(3), 2037–2056. https://doi.org/10.1002/2017WR022257

Moore, W. S. (2010). The effect of submarine groundwater discharge on the ocean. *Annual Review of Marine Science*, *2*(1), 59–88. https://doi.org/10.1146/annurev-marine-120308-081019

Nielsen, P. (1990). Tidal dynamics of the water table in beaches. *Water Resources Research*, *26*(9), 2127–2134. https://doi.org/10.1029/WR026i009p02127

Nielsen, P., Aseervatham, R., Fenton, J. D., & Perrochet, P. (1997). Groundwater waves in aquifers of intermediate depths. *Advances in Water Resources*, *20*(1), 37–43. https://doi.org/10.1016/S0309-1708(96)00015-2

Nielsen, P., & Perrochet, P. (2000). Watertable dynamics under capillary fringes: Experiments and modelling. *Advances in Water Resources*, *23*(5), 503–515. https://doi.org/10.1016/S0309-1708(99)00038-X

Parlange, J.-Y., Stagnitti, F., Heilig, A., Szilagyi, J., Parlange, M. B., Steenhuis, T. S., Hogarth, W. L., Barry, D. A., & Li, L. (2001). Sudden drawdown and drainage of a horizontal aquifer. *Water Resources Research*, *37*(8), 2097–2101. https://doi.org/10.1029/2000WR000189

Parlange, J.-Y., Stagnitti, F., Starr, J. L., & Braddock, R. D. (1984). Free-surface flow in porous media and periodic solution of the shallow-flow approximation. *Journal of Hydrology*, *70*(1–4), 251–263. https://doi.org/10.1016/0022-1694(84)90125-2

Parlange, J.-Y., & Brutsaert, W. (1987). A capillarity correction for free surface flow of groundwater. *Water Resources Research*, *23*(5), 805–808. https://doi.org/10.1029/WR023i005p00805

Philip, J. R. (1973). Periodic nonlinear diffusion: An integral relation and its physical consequences. *Australian Journal of Physics, 26*(4), 513–520. https://doi.org/10.1071/PH730513

Pozdniakov, S. P., Wang, P., & Lekhov, V. A. (2019). An approximate model for predicting the specific yield under periodic water table oscillations. *Water Resources Research*, *55*(7), 6185–6197. https://doi.org/10.1029/2019WR025053

Rabinovich, A., Barrash, W., Cardiff, M., Hochstetler, D. L., Bakhos, T., Dagan, G., & Kitanidis, P. K. (2015). Frequency dependent hydraulic properties estimated from oscillatory pumping tests in an unconfined aquifer. *Journal of Hydrology*, *531*, 2–16. https://doi.org/10.1016/j.jhydrol.2015.08.021

Raubenheimer, B., Guza, R. T., & Elgar, S. (1999). Tidal water table fluctuations in a sandy ocean beach. *Water Resources Research*, *35*(8), 2313–2320. https://doi.org/10.1029/1999WR900105

Robinson, C., Gibbes, B., & Li, L. (2006). Driving mechanisms for groundwater flow and salt transport in a subterranean estuary. *Geophysical Research Letters*, *33*(3), L03402. https://doi.org/10.1029/2005GL025247

Robinson, C., & Li, L. (2004). Effect of tidal oscillations on water exchange and mixing in a coastal aquifer. *Developments in Water Science*, 55(Part 2), 1583–1594.

https://doi.org/10.5194/hess-2021-634
Preprint. Discussion started: 18 January 2022

https://doi.org/10.1016/S0167-5648(04)80168-0

Robinson, C., Li, L., & Barry, D. A. (2007). Effect of tidal forcing on a subterranean estuary. *Advances in Water Resources*, *30*(4), 851–865. https://doi.org/10.1016/j.advwatres.2006.07.006

Robinson, C., Xin, P., Li, L., & Barry, D. A. (2014). Groundwater flow and salt transport in a subterranean estuary driven by intensified wave conditions. *Water Resources Research*, *50*(1), 165–181. https://doi.org/10.1002/2013WR013813

Robinson, C. E., Xin, P., Santos, I. R., Charette, M. A., Li, L., & Barry, D. A. (2018). Groundwater dynamics in subterranean estuaries of coastal unconfined aquifers: Controls on submarine groundwater discharge and chemical inputs to the ocean. *Advances in Water Resources*, *115*, 315–331. https://doi.org/10.1016/j.advwatres.2017.10.041

Shen, Y., Xin, P., & Yu, X. (2020). Combined effect of cutoff wall and tides on groundwater flow and salinity distribution in coastal unconfined aquifers. *Journal of Hydrology*, *581*, 124444. https://doi.org/10.1016/j.jhydrol.2019.124444

Shoushtari, S. M. H. J., & Cartwright, N. (2017). Modelling the effects of porous media deformation on the propagation of water-table waves in a sandy unconfined aquifer. *Hydrogeology Journal*, *25*(2), 287–295. https://doi.org/10.1007/s10040-016-1487-7

Shoushtari, S. M. H. J., Cartwright, N., Nielsen, P., & Perrochet, P. (2016). The effects of oscillation period on groundwater wave dispersion in a sandy unconfined aquifer: Sand flume experiments and modelling. *Journal of Hydrology*, *533*, 412–420.

https://doi.org/10.5194/hess-2021-634
Preprint. Discussion started: 18 January 2022

https://doi.org/10.1016/j.jhydrol.2015.12.032

Shoushtari, S. M. H. J., Cartwright, N., Perrochet, P., & Nielsen, P. (2015). Influence of hysteresis on groundwater wave dynamics in an unconfined aquifer with a sloping boundary. *Journal of Hydrology*, *531*, 1114–1121. https://doi.org/10.1016/j.jhydrol.2015.11.020

Shoushtari, S. M. H. J., Cartwright, N., Perrochet, P., & Nielsen, P. (2017). Two-dimensional vertical moisture-pressure dynamics above groundwater waves: Sand flume experiments and modelling. *Journal of Hydrology*, *544*, 467–478. https://doi.org/10.1016/j.jhydrol.2016.11.060

Šimůnek, J., van Genuchten, M. Th., & Šejna, M. (2020). *The HYDRUS software package for simulating the two-and three-dimensional movement of water, heat, and multiple solutes in variably-saturated porous media. Technical Manual*. https://www.pc-progress.com/downloads/Pgm_Hydrus3D3/HYDRUS3D_Technical_Manual_V3.pdf, last accessed 18 March 2021

Smiles, D. E., & Stokes, A. N. (1976). Periodic solutions of a nonlinear diffusion equation used in groundwater flow theory: Examination using a Hele-Shaw model. *Journal of Hydrology, 31*(1–2), 27–35. https://doi.org/10.1016/0022-1694(76)90018-4

Song, Z., Li, L., Kong, J., & Zhang, H. (2007). A new analytical solution of tidal water table fluctuations in a coastal unconfined aquifer. *Journal of Hydrology*, *340*(3–4), 256–260. https://doi.org/10.1016/j.jhydrol.2007.04.015

Teo, H. T., Jeng, D. S., Seymour, B. R., Barry, D. A., & Li, L. (2003). A new analytical solution for water table fluctuations in coastal aquifers with sloping beaches. *Advances in Water Resources*, *26*(12), 1239–1247. https://doi.org/10.1016/j.advwatres.2003.08.004

Trglavcnik, V., Morrow, D., Weber, K. P., Li, L., & Robinson, C. E. (2018). Analysis of tide and offshore storm-induced water table fluctuations for structural characterization of a coastal island aquifer. *Water Resources Research*, *54*(4), 2749–2767. https://doi.org/10.1002/2017WR020975

Troch, P. (1993). *Conceptual basin-scale runoff process models for humid catchments: Analysis, synthesis and applications*. RUG. Faculteit Landbouwkundige en Toegepaste Biologische Wetenschappen. http://hdl.handle.net/1854/LU-8566676, last accessed 18 March 2021

van Genuchten, M. Th. (1980). A closed-form equation for predicting the hydraulic conductivity of unsaturated soils. *Soil Science Society of America Journal*, *44*(5), 892–898. https://doi.org/10.2136/sssaj1980.03615995004400050002x

Voss, C. I., & Provost, A. M. (2008). *SUTRA: A model for saturated-unsaturated, variable density groundwater flow with solute or energy transport*. Reston, VA: U.S. Geological Survey. https://water.usgs.gov/nrp/gwsoftware/sutra/SUTRA_2_2-documentation.pdf, last accessed 28 December 2021

Voss, C. I., & Souza, W. R. (1987). Variable density flow and solute transport simulation of regional aquifers containing a narrow freshwater-saltwater transition zone. *Water Resources Research*, *23*(10), 1851–1866. https://doi.org/10.1029/WR023i010p01851

https://doi.org/10.5194/hess-2021-634
Preprint. Discussion started: 18 January 2022

Wallace, C. D., Sawyer, A. H., Soltanian, M. R., & Barnes, R. T. (2020). Nitrate removal within heterogeneous riparian aquifers under tidal influence. *Geophysical Research Letters*, *47*(10), e2019GL085699. https://doi.org/10.1029/2019GL085699

Werner, A. D., Bakker, M., Post, V. E. A., Vandenbohede, A., Lu, C., Ataie-Ashtiani, B., Simmons, C. T., & Barry, D. A. (2013). Seawater intrusion processes, investigation and management: Recent advances and future challenges. *Advances in Water Resources*, *51*, 3–26. https://doi.org/10.1016/j.advwatres.2012.03.004

Xin, P., Robinson, C., Li, L., Barry, D. A., & Bakhtyar, R. (2010). Effects of wave forcing on a subterranean estuary. *Water Resources Research*, *46*(12), W12505. https://doi.org/10.1029/2010WR009632

Yu, X., Xin, P., & Lu, C. (2019). Seawater intrusion and retreat in tidally-affected unconfined aquifers: Laboratory experiments and numerical simulations. *Advances in Water Resources*, *132*, 103393. https://doi.org/10.1016/j.advwatres.2019.103393

Zhang, Y., Li, L., Erler, D. V., Santos, I., & Lockington, D. (2016). Effects of alongshore morphology on groundwater flow and solute transport in a nearshore aquifer. *Water Resources Research*, *52*(2), 990–1008. https://doi.org/10.1002/2015WR017420

https://doi.org/10.5194/hess-2021-634
Preprint. Discussion started: 18 January 2022

Hydrology and Earth System Sciences
Open Access
Discussions

Table 1. Soil properties for watertable fluctuation and seawater intrusion experiments.

	K_s (m/s)	n_e	α^{c} (m^{-1})	n^{c}	α_1 (m^{-1})	n_1	H_ψ (m)
Watertable fluctuation[a]	4.7×10^{-4}	0.32	1.7	9	1.63	8.27	0.61
Seawater intrusion[b]	3×10^{-3}	0.4	11	6	10	5.23	0.1

[a]Compiled from Shoushtari et al. (2016)

[b]Compiled from Shen et al. (2020)

[c]α and n are the VG fitting parameters (van Genuchten, 1980)

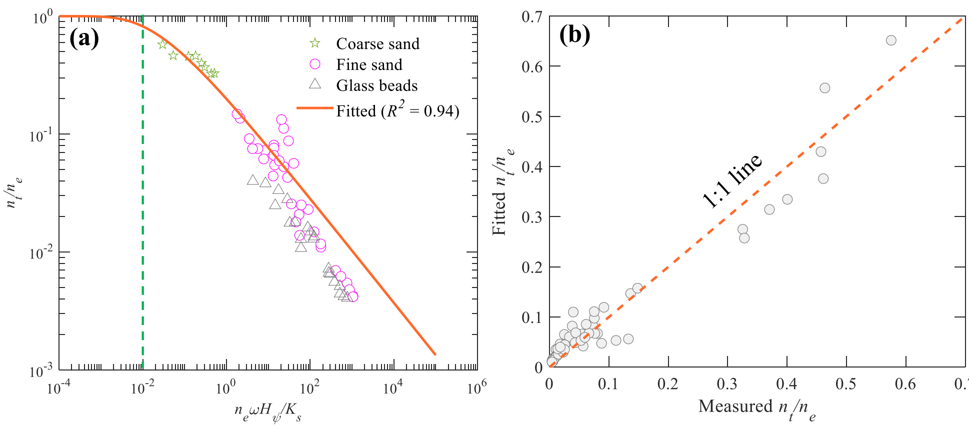

Figure 1. (a) Comparison of experimental and fitted relations between n_t/n_e and τ_ω. Note that the green dashed line indicates the critical value (about 0.01) when the effective porosity will be significantly impacted by watertable fluctuations. (b) Fitted n_t/n_e versus experimental n_t/n_e. Experimental data are compiled from Cartwright et al. (2005).

https://doi.org/10.5194/hess-2021-634
Preprint. Discussion started: 18 January 2022

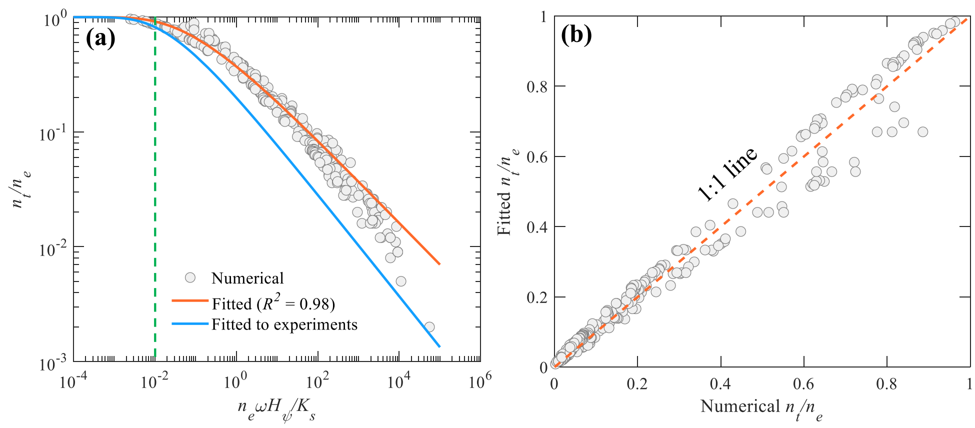

Figure 2. (a) Comparison of numerical and fitted relations between n_t/n_e and τ_ω. Note that the green dashed line indicates the critical value (about 0.01) when the effective porosity will be significantly impacted by watertable fluctuations and the blue line is fitted to experimental data of Cartwright et al. (2005). (b) Fitted n_t/n_e versus numerical n_t/n_e. Numerical data are compiled from Pozdniakov et al. (2019).

https://doi.org/10.5194/hess-2021-634
Preprint. Discussion started: 18 January 2022

Hydrology and Earth System Sciences
Open Access
Discussions

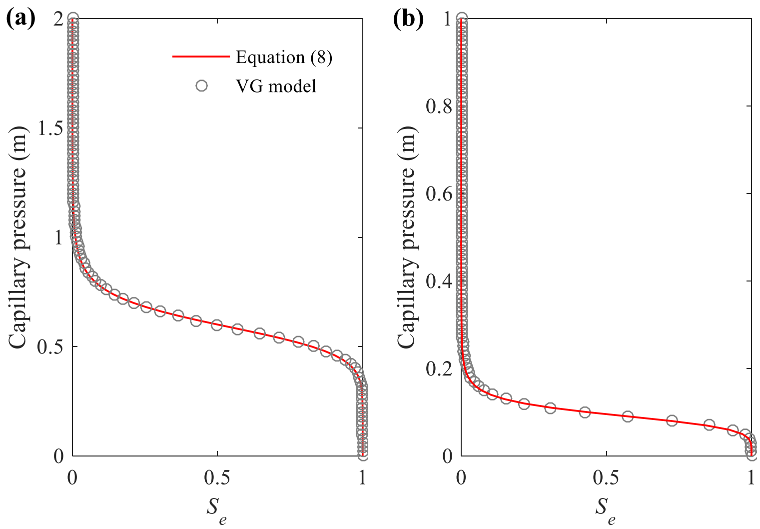

Figure 3. Comparison between equation (8) and the VG model for the soil adopted in (a) watertable fluctuation and (b) seawater intrusion experiments. Data are compiled from Shoushtari et al. (2016) and Shen et al. (2020), respectively

https://doi.org/10.5194/hess-2021-634
Preprint. Discussion started: 18 January 2022

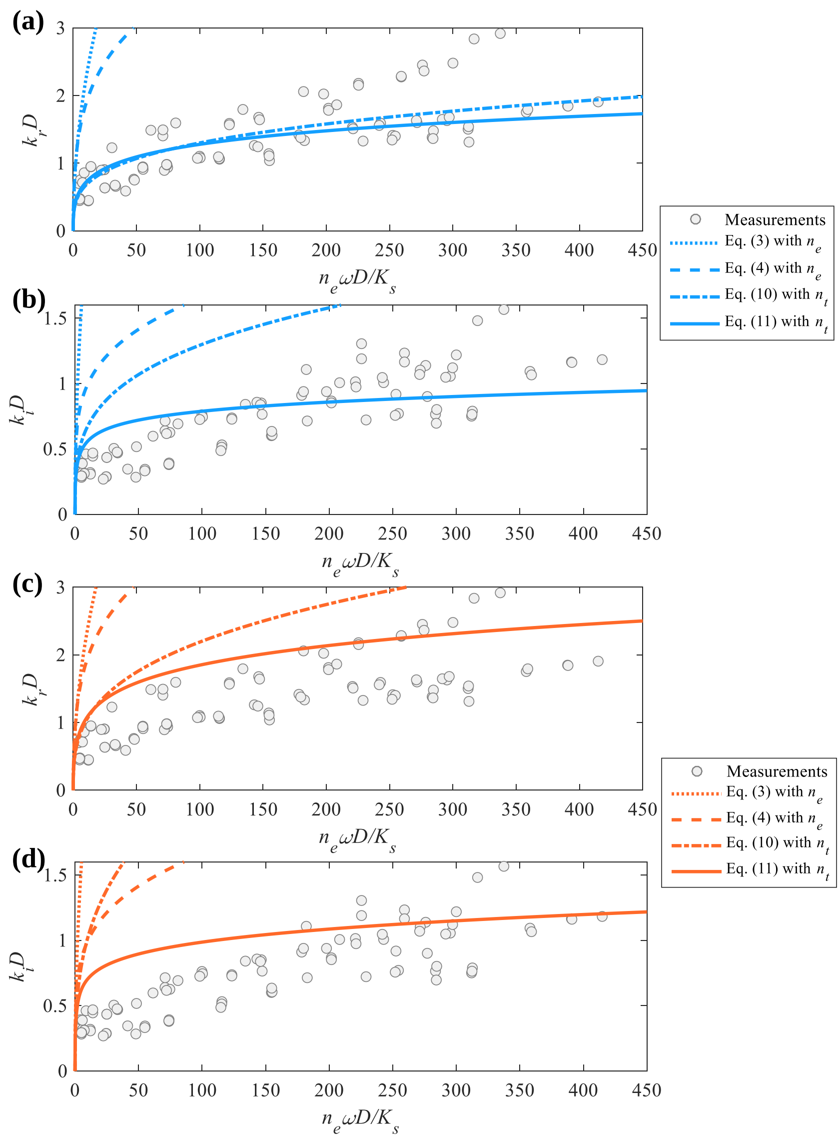

Figure 4. Comparison model predictions and experimental results of (a, c) amplitude decay rate (k_rD) and (b, d) phase lag increase rate (k_iD) versus $n_e\omega D/K_s$. The values of a and b used for the blue lines and orange lines are based on the experiments (a = 0.0335, b = 0.4444) and numerical simulations (a = 0.1216, b = 0.3642), respectively. Parameters used are consistent with Shoushtari et al. (2016): D = 0.92 m, H_ψ = 0.61 m and K_s = 4.7 × 10^{-4} m/s.

https://doi.org/10.5194/hess-2021-634
Preprint. Discussion started: 18 January 2022

Hydrology and Earth System Sciences
Open Access
Discussions

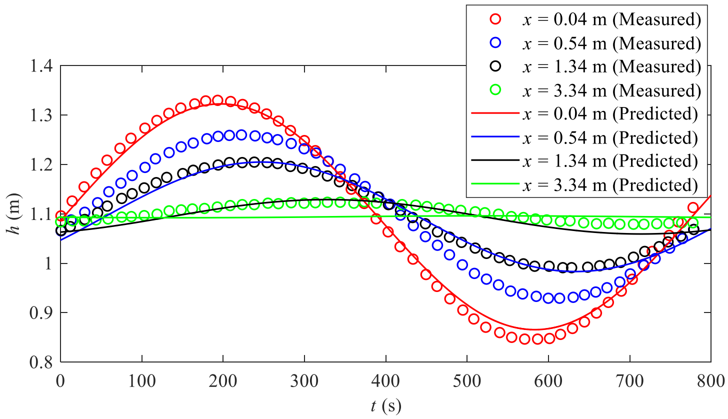

744

745 **Figure 5.** Comparison of measured watertable and predictions from equation (11).

746 Experimental data are compiled from Parlange et al. (1984). Since n_e and K_s were not

747 measured in the experiments of Parlange et al. (1984), the optimal value of n_t/K_s in equation

748 (11) was estimated to be 0.5 s/cm based on the measured watertable at different locations.

https://doi.org/10.5194/hess-2021-634
Preprint. Discussion started: 18 January 2022

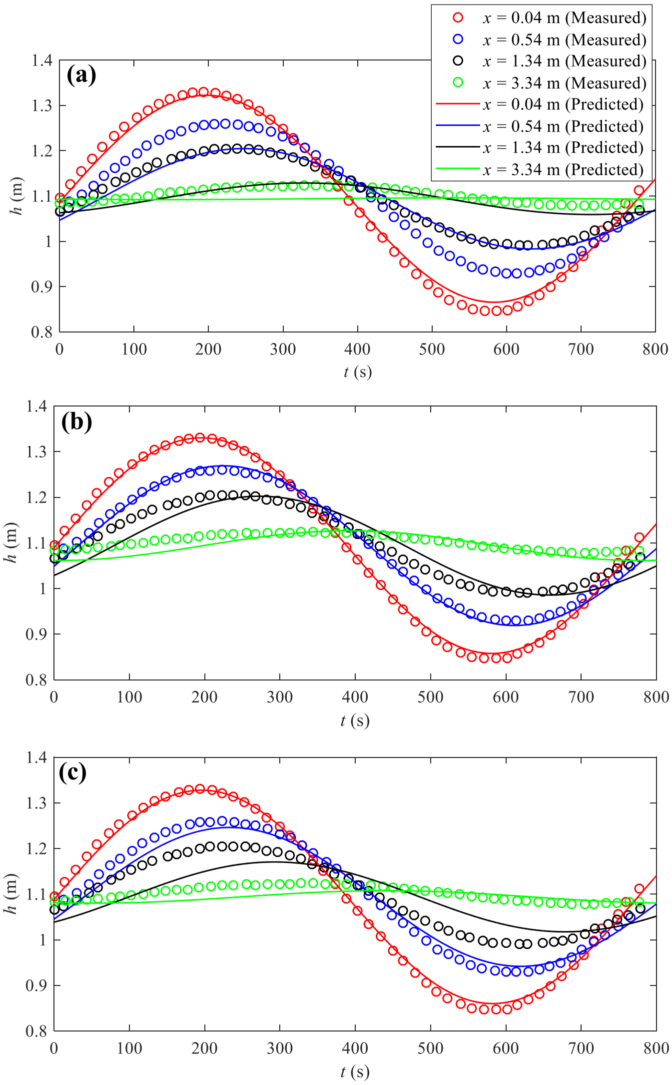

Figure 6. Comparison of measured watertable and predictions from (a) equation (2) (ignoring the dynamic effective porosity), (b) equation (11) with $a = 0.0335$ and $b = 0.4444$, and (c) equation (11) with $a = 0.1216$ and $b = 0.3642$. Experimental data are compiled from Cartwright et al. (2003).

https://doi.org/10.5194/hess-2021-634
Preprint. Discussion started: 18 January 2022

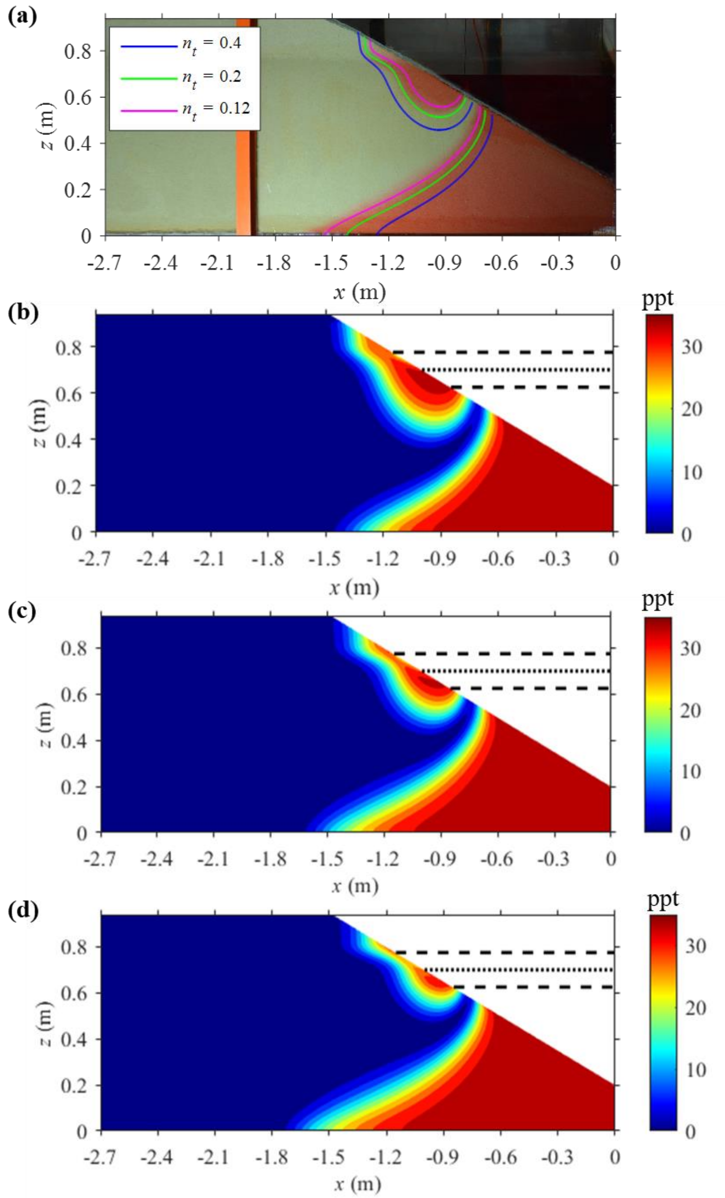

Figure 7. Comparison of (a) measurements (Shen et al., 2020) and numerical results (quasi-steady state) with (b) $n_t = 0.4$ (equal to n_e), (c) $n_t = 0.2$ and (d) $n_t = 0.12$. Three lines in plot (a) are simulated 50% isohalines corresponding to three cases respectively. In plots (b)-(c), the

https://doi.org/10.5194/hess-2021-634
Preprint. Discussion started: 18 January 2022

upper and bottom dashed lines indicate the highest and lowest water levels, respectively, and the middle dotted line represents the mean water level.